A combined photobiological-photochemical route to C_{10} cycloalkane jet fuels from carbon dioxide *via* isoprene†

Anup Rana,[a] Leandro Cid Gomes,[a] João S. Rodrigues,[a] Hugo Arrou-Vignod,[a] Johan Sjölander,[a] Nathalie Proos Vedin,[a] Ouissam El Bakouri,[a] Karin Stensjö,[a] Peter Lindblad,[a] Leena Andersson,[b] Mathias Berglund,[b]* Pia Lindberg [a]* and Henrik Ottosson [a]*

[a] Department of Chemistry – Ångström Laboratory, Uppsala University, Box 523, 751 20 Uppsala, Sweden.

Email: henrik.ottosson@kemi.uu.se, pia.lindberg@kemi.uu.se

[b] RISE Research Institutes of Sweden, Brinellgatan 4, Box 857, 501 15 Borås, Sweden.

Email: mathias.berglund@ri.se

† Electronic supplementary information (ESI) available.

Abstract: The hemiterpene isoprene is a volatile C_5 hydrocarbon, with industrial applications. It is generated today from fossil resources, but can also be made in biological processes. We have utilized engineered photosynthetic cyanobacteria for direct, light-driven production of bio-isoprene from carbon dioxide, and show that isoprene in a subsequent photochemical step, using simulated or natural solar light, can be dimerized into limonene, paradiprene, and isomeric $C_{10}H_{16}$ hydrocarbons (monoterpenes) in very high yields (above 90% after 44 hours) under sensitized conditions. The optimal sensitizer in our experiments is di(naphth-1-yl)methanone which we can use with a loading of merely 0.1 mol%, and it is easily recycled for subsequent photodimerization cycles. The isoprene dimers generated are a mixture of [2+2], [4+2] and [4+4] cycloadducts, and after hydrogenation this mixture is nearly ideal as a jet fuel drop-in.

Importantly, the photodimerization can be carried out at ambient conditions. The high content of hydrogenated [2+2] dimers in our isoprene dimer mix lowers the flash point below the threshold (38 °C), yet, these dimers can be converted thermally into [4+2] and [4+4] dimers. When hydrogenated these monoterpenoids fully satisfy the criteria for drop-in jet fuels with regard to energy density, flashpoint, kinematic viscosity, density, and freezing point.

TOC graphic:

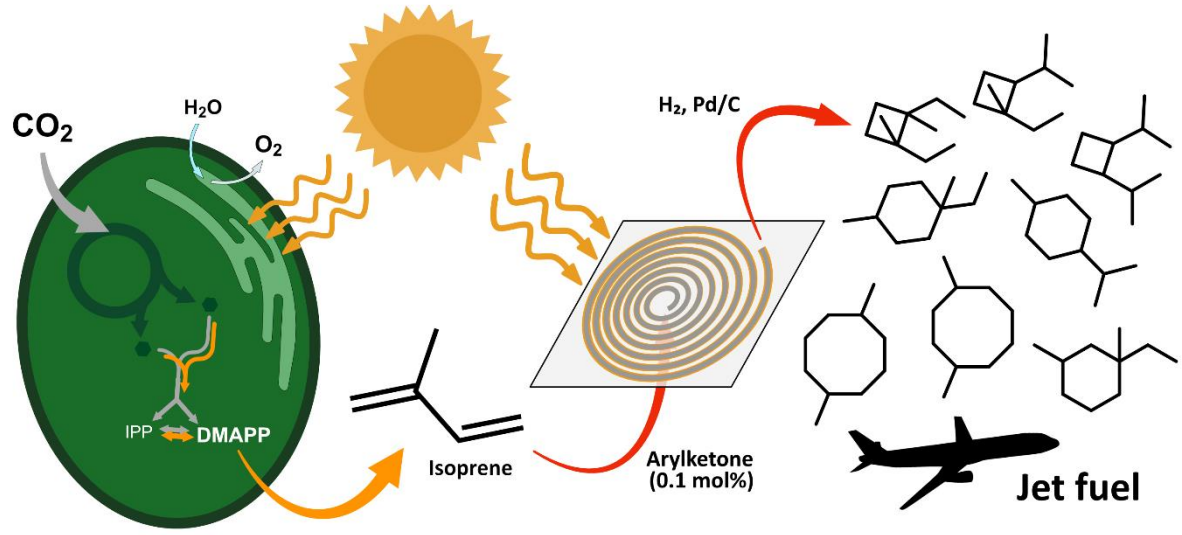

Broader Context: The transportation sector is one of the major contributors to greenhouse gas emission due to the use of fossil-based fuels. While the automobile industry is slowly shifting towards electric vehicles, the aviation sector is still dependent of fossil fuels. To mitigate the environmental effect, biofuels have been introduced (in early stage of development) in the aviation sector. However, the biofuels production is dependent on biomass as a source of raw material which leads to competition with farmland and to rapid deforestation. Therefore, technology is needed to utilize CO_2 as substrate for production of jet fuels, in a true carbon neutral process. Here, we report a combined photobiological and photochemical process for

production of jet fuel equivalents, using CO_2 as source of carbon and light as source of energy. A small hydrocarbon, isoprene, is produced by engineered photosynthetic cyanobacteria, and subsequently converted to C_{10} cycloalkanes by a photochemical process followed by catalytic hydrogenation. The C_{10} cycloalkane blends have all attributes to be used as drop-in jet fuels, ultimately enabling usage of the presently available infrastructure for aviation fuels.

Keywords: Aviation fuels, cyanobacteria, DFT computations, isoprene, solar fuels, triplet sensitizer

Introduction

In order to mitigate global warming and reach the goals of the Paris agreement, a move to usage of carbon neutral fuels is necessary. For year 2050, the International Air Transport Association (IATA) emission reduction roadmap projects a reduction in CO_2 emissions from aviation by 50% compared to 2005 levels.[1] This may seem modest, yet, globally air traffic increased by 4.5 – 8.7% per year during the period 2009 – 2018,[2] and a low annual increase of 4% until 2050, resulting from changes in travel patterns due to covid-19 and the installment of alternative transportation infrastructures, still implies more than a three-fold increase in air traffic by 2050 when compared to 2018 and approximately six-fold when compared to 2005. As the increase in air traffic is often considerably steeper in growing economies, fulfilment of the IATA goal requires prompt technological development and introduction of new sustainable aviation fuels far beyond the biofuels currently in use or at the stage to be introduced on the market.

Today, there are different technologies and feedstock alternatives to conventional jet fuels. An emerging route to biofuels goes via direct production of hydrocarbons by engineered photosynthetic microorganisms, such as algae or cyanobacteria. Cyanobacteria are photosynthetic bacteria which grow on water, minerals, and CO_2 from the atmosphere, using

sunlight as their energy source. Many cyanobacterial strains are amenable to genetic engineering, and thus, they are ideal hosts for biotechnological production of sustainable fuels.[3]

Fossil-based jet fuels consist mostly of C_8 - C_{16} hydrocarbons. More explicitly, they are mixtures of n-, iso- and cyclo-alkanes, small aromatics (< 25%) and alkenes (< 5%).[4,5] The fuel should be a proportional mixture of these compounds in order to follow the strict requirement for jet-fuels in terms of energy density, freezing point, and viscosity. In one typical jet fuel, JP-8, the proportion of C_{10} hydrocarbons is ~21%.[6] Hydrogenated monoterpenes (C_{10}) and sesquiterpenes (C_{15}) have long been considered as potential jet fuels due to their low viscosity and high energy density. Limonane (hydrogenated limonene) has been in focus among hydrogenated monoterpenes because of its availability from biomass fermentation and the low estimated cost of the resulting fuel (~0.73 USD/lit).[7] Sesquiterpenes, *e.g.* bisabolene and epi-isozizaene, are also molecules with potential utility.[7–9]

Yet, while biotechnological production of monoterpenes and sesquiterpenes in various microorganisms have been demonstrated, the toxicity of these compounds to the cells is often problematic. Mono- and sesquiterpenoids tend to accumulate in the biological membranes, due to their hydrophobic nature, and interfere with their integrity and function.[5] On the other hand, smaller hydrocarbons, *e.g.*, alkenes such as *iso*-butene and the 5-carbon-atom hemiterpenoids, are more volatile and tend to easily escape through the cell membranes.[10,11] Their diffusion to the extracellular environment makes them less toxic to the cells and their harvest/capture is less costly since there is no need for cell disruption. We therefore suggest a two-step procedure in which these small volatile hydrocarbons (C_5 and smaller) are produced photobiologically, followed by their photochemical oligomerization in a second separate step. Isoprene is a volatile five-carbon hydrocarbon and can be an ideal precursor. It contains CC double bonds which are useful as sites for (photo)oligomerization, and its production by photosynthetic engineered cyanobacteria has been demonstrated.[10,12,13]

Thus, hydrogenated isoprene oligomers could be ideal as drop-ins into presently used aviation fuels.

Although there are already well-established chemical methods using heterogeneous catalysts used in the industry for oligomerization of alkenes and dienes,[14] these methods require high temperatures and pressures. More energy-efficient procedures are desirable. Recently, Harvey and co-workers reported iron-catalyzed dimerization processes of alkenes and dienes, including isoprene, that run at ambient temperature and pressure and that produce [2+2] and [4+4] cycloadducts (Fig. 1).[15,16] Interestingly, the hydrogenated [4+4] dimers of isoprene have better fuel properties compared to conventional jet fuels (Jet-A). Although the products after hydrogenation are suitable as jet fuels, the catalysts are highly air-sensitive and the reactions had to be run under inert atmospheric conditions. Furthermore, the [2+2] oligomerization of isoprene required two weeks and resulted in dimers, trimers and tetramers. We reason that the selective formation of one specific oligomer type, even if in a mixture of isomers, under ambient conditions should be preferable.

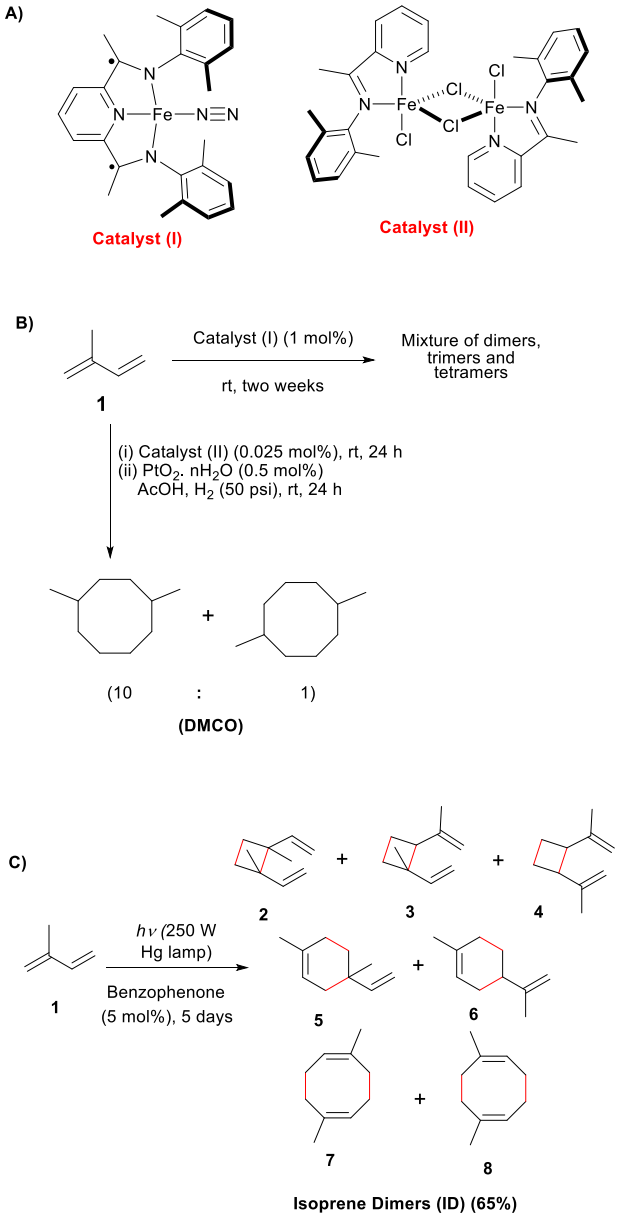

Figure 1: A) The two iron-based catalysts by Harvey and co-workers,[15,16] and B) the catalyzed oligomerization of isoprene. C) Photochemical dimerization of isoprene which resulted in the formation of [2+2], [4+2] and [4+4] photodimers.[17] Bonds formed in the reaction are marked in red.

We have explored to what extent isoprene can be dimerized photochemically through triplet sensitizers using as mild conditions as possible, ultimately with solar light and in ambient atmosphere. The photochemical dimerization of isoprene was reported already in

the 60s by Hammond, Turro and Liu using benzophenone (5 mol%) as photosensitizer (Fig. 1C), leading to 65% conversion to isoprene dimers when irradiated for five days in a sealed tube (irradiation with a 250 W Hannovia Hg lamp with 280 nm cutoff filter).[17] Interestingly, the composition of the dimer mixtures, *i.e.*, the distribution of [2+2], [4+2] *vs.* [4+4] cycloadducts, depended on the triplet energies of photosensitizers,[18] yet importantly, trimers and longer oligomers were not formed. Combined with photosynthetic generation of isoprene from CO_2, this could provide for sustainable production of hydrocarbons for jet fuels. However, there are very few results towards the direct production of jet fuels from CO_2.[19–21] Most of these methods required complex metal catalysts in addition to high temperature or/and pressure. Therefore, the process to convert CO_2 to jet fuel in a greener way, ideally at ambient condition, should be more desirable. Hence, we now report on the first formation of C_{10} hydrocarbons, suitable as jet fuel drop-ins, in a combined two-step photobiological-photochemical approach with CO_2 as carbon source and with light, either as (simulated) solar or ambient light, as the energy source.

Results and Discussion

The photobiological formation and trapping of the isoprene produced by the cyanobacteria are presented first, followed by optimization of the photoinitiated dimerization of isoprene (including bio-isoprene) to yield C_{10} hydrocarbons (monoterpenoids). The dimerization mechanism is analyzed through density functional theory (DFT) computations, unravelling why isoprene trimers are only formed in trace amounts. To be useful as a fuel, the monoterpenoids formed need to be hydrogenated, and we determine various properties and assess the values of our hydrogenated monoterpenoids in relation to what is required for a jet fuel.

Microbial production and trapping of isoprene: Cyanobacteria, like other bacteria, are able to generate terpenoids via the methylerythritol-4-phosphate (MEP) pathway, but do not naturally produce isoprene (Fig. 2A).[22] In previous work, we have established engineered strains of the unicellular cyanobacterium *Synechocystis* sp. PCC 6803 (hereafter *Synechocystis*), capable of light-driven isoprene production from CO_2, via photosynthesis. This was achieved through the introduction of genes encoding an efficient isoprene synthase (IspS) and two enzymes upstream in the MEP pathway - DXS, 1-deoxy-D-xylulose-5-phosphate synthase, and IDI, isopentenyl-diphosphate isomerase (Fig. 2A).[13] DXS performs the first step of the pathway by combining the two substrates pyruvate and glyceraldehyde-3-phosphate to form 1-deoxy-D-xylulose 5-phosphate (DXP). IDI performs the interconversion of isopentenyl diphosphate (IPP) and dimethylallyl diphosphate (DMAPP), the substrate for the isoprene synthase to form isoprene.[13,22] The reaction catalyzed by DXS includes a decarboxylation step, thereby serving as a gateway for the flux of carbon into the MEP pathway. The expression of IDI is likely necessary to maintain the balance between IPP and DMAPP, and thus enable the synthesis of essential terpenoids downstream in the terpenoid biosynthesis, when IspS expression would otherwise deplete the levels of DMAPP in the cell.[13]

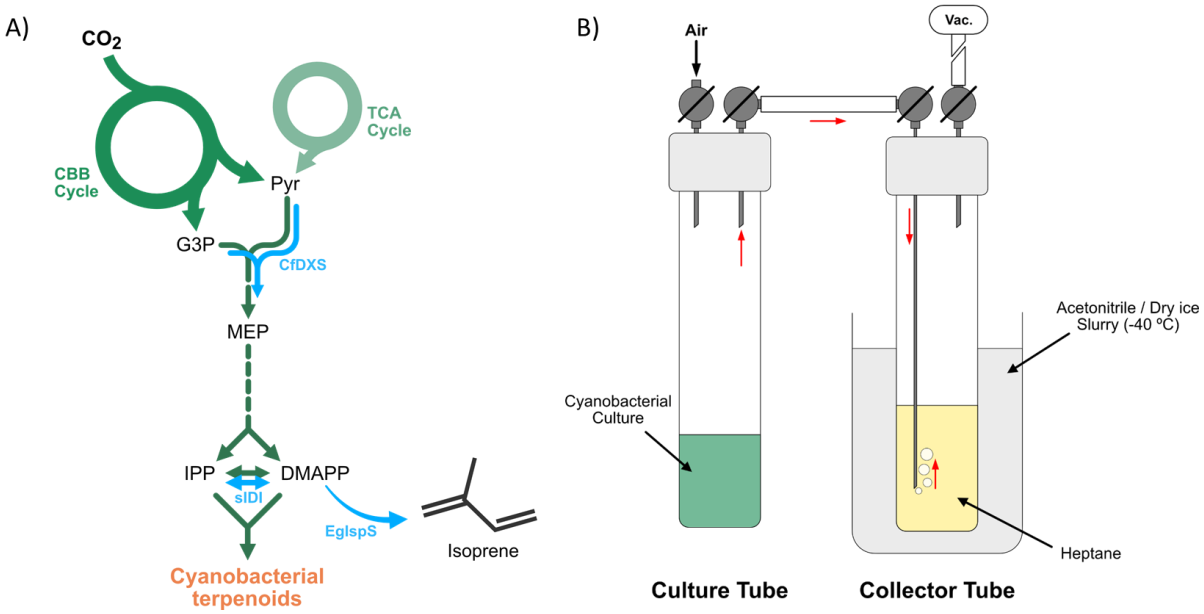

Fig. 2 A) Schematic representation of cyanobacterial terpenoid pathway (green) and genetic modifications (blue arrows) in the isoprene-producing strain used in this study. B) Schematic representation of the customized isoprene capturing system. CBB - Calvin-Benson-Bassham; TCA - tricarboxylic acid; Pyr - pyruvate; G3P - glyceraldehyde-3-phosphate; MEP - methylerythritol-4-phosphate; IPP - isopentenyl-pyrophosphate; DMAPP - dimethylallyl-pyrophosphate; CfDXS - 1-deoxy-D-xylulose-5-phosphate synthase from *Coleus forskohlii*; sIDI - IPP/DMAPP isomerase from *Synechocystis* sp. PCC 6803; EgIspS - isoprene synthase from *Eucalyptus globulus*. Vac = vacuum line. The red arrows indicate the flow of the isoprene vapor.

Here, we have used the engineered *Synechocystis* cells for photosynthetic production of isoprene in small-scale bioreactors. 20 ml of cyanobacterial culture were grown for four days in sealed 60 ml culture tubes under a constant illumination of 50 µmol photons m^{-2} s^{-1}, with addition of 50 mM $NaHCO_3$ to the culture medium. Thereafter, the headspace gas was drawn through 20 ml of cold heptane to capture produced bio-isoprene from the cultures (Fig. 2B). Isoprene concentrations in the gas phase of the cultures were determined by gas

chromatography comparing to an isoprene standard, before and after capturing of the gas phase. For further experimental details, see Fig. S1, ESI†.

We achieved an isoprene titre of 1.60 mg L^{-1} culture after four days of cultivation under the abovementioned conditions. After capturing the isoprene in heptane in our customized trapping setup, the equivalent of 935 µg L^{-1} of culture remained in the cultivation tube, which translates into a capture efficiency of 41.4% (Fig. S2, ESI† and Table S1, ESI†). A second cycle of trapping resulted in the capture of *ca.* 490 µg L^{-1} culture and a higher efficiency (52.4%), for a combined trapping efficiency of ca 70%. Throughout the experiments, there was variability in the isoprene production by the engineered strain, likely due to genetic instability of the expression constructs. Such problems can be overcome by further optimization of the strain engineering (*e.g.* integration of the synthetic device into the cyanobacterial chromosome). Additionally, we achieved higher capture efficiencies in a single trapping step for other tests, reaching as high as 89% of the isoprene produced. The bio-isoprene trapped in the heptane of the collector tubes was then used for the photochemical dimerization experiments (see section below on *Photodimerization of bio-isoprene*).

Screening of triplet sensitizers: To establish a photochemical dimerization process that utilizes solar irradiation (natural or simulated) we started at the triplet sensitized diene dimerization reported by Hammond, Turro and Liu in the 60s.[17] Arylketones are excellent photosensitizers due to their relatively high triplet quantum yield and exceptional photostability. The excitation wavelength of arylketones can be tuned to the visible region by extension of π-conjugation of the aryl groups. Additionally, the triplet quantum yield of ketones can be greatly improved compared to the corresponding arene chromophore.[23] Such modulations push the excitation of the sensitizers toward the visible wavelength region where they can be activated by solar light (see below). In the screening of photosensitizers suitable for photodimerization of isoprene we used benzophenone (**9**), xanthone (**10**), thioxanthone (**11**),

di(naphth-1-yl)methanone (**12**), naphthalen-1-yl(naphth-2-yl)methanone (**13**), and di(naphth-2-yl)methanone (**14**), see Fig. 3. The synthesis of the photosensitizers is discussed in the ESI†. The $E(T_1)$'s of **9 - 14** and isoprene, both experimentally determined and calculated, indicate that these ketones are suitable for effective photosensitization because their $E(T_1)$'s are slightly higher than that of isoprene (Fig. 3 and Fig. S3, ESI†). Furthermore, their T_1 states are of ππ* character which prevents the competing H atom abstraction,[24] a photoreaction that many ketones with nπ* states initiate. In a typical photoreaction, a mixture of inhibitor-free isoprene and aryl ketone was contained in a quartz test tube under argon and irradiated with 365 nm light (Fig. S4, ESI†). The solution was stirred during the photoirradiation in order to achieve uniform light exposure.

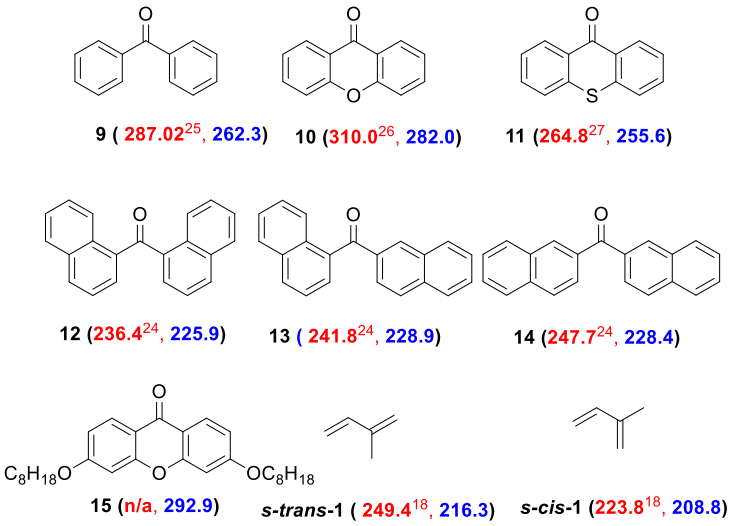

Fig. 3 The photosensitizers used in this study as well as isoprene, and in parenthesis, their experimental triplet energies (kJ/mol, in red) and the calculated adiabatic triplet energies (in blue) at (U)B3LYP-D3/6-311+G(d,p) level.[18,24–27]

The isoprene dimers formed were characterized by ^{1}H NMR spectroscopy and gas chromatography-mass spectrometry (GCMS) analysis (Fig. S5 - S8, ESI†). However, we confirmed the structure of the isomers by ^{1}H NMR spectroscopy as the GC chromatograms can

give erroneous results on the relative product distribution due to thermal rearrangement of the dimers (see below). Seven isomeric isoprene dimers (**2 – 8**) were observed, in line with findings reported by Hammond, Turro and Liu (Fig. 1C and Fig. S8, ESI†).[17] It was also proposed by Hammond and Liu that cyclooctadienes **7** and **8** might have resulted from thermal rearrangements in the GC,[28] but our ^{1}H NMR data of the isoprene dimers (purified by silica gel column by using pentane as eluent) reveals that these two dimers originate from photoinitiated dimerization and cyclization. Here it can be noted that the distribution of the various isomers depends on the $E(T_1)$'s of the photosensitizers used. It is also noteworthy that trace amounts of isoprene trimers were formed, but not any longer oligomers (Fig. S6, ESI†).

The screening of the photosensitizers was performed by using 2 mol% loading, unless otherwise mentioned in Table 1. Depending on the photosensitizer, with the quartz tube setup (Fig. S4, ESI†) we observed 8 - 41% conversion to isoprene dimers with di(naphthalen-1-yl)methanone **12** giving the highest conversion. A control experiment carried out without photosensitizer clarified its crucial role as the conversion dropped to 0.5% after 44 h of irradiation with λ = 365 nm. The isoprene dimers formed in this case presumably arise from thermal Diels-Alder reactions because [4+2] cycloadducts were observed as the major products (Fig. S9, ESI†).

Interestingly, the efficiency of the three dinaphthylmethanone isomers to convert isoprene to its dimers varied from 21 to 41% due to the positional effect of naphthyl groups. Thus, one dinaphthylmethanone (**12**) acts as a better photosensitizer than benzophenone, another one (**13**) performs similarly, and a third one (**14**) performs worse. If we compare the relative absorbance of the benzophenone and the three dinaphthylmethanone isomers at 365 nm, the maximum molar extinction coefficient is observed for **13** and minimum for **9** (Fig. S10-11, ESI†), and from the $E(T_1)$'s of **12** – **14** (Fig. 3) it is clear that **12** is the dinaphthylmethanone with a triplet energy closest to that of isoprene. Additionally, the absorption tails of the

dinapthylmethanones go beyond 400 nm, which possibly enable solar light photosensitization. Finally, both **12** and **13** have triplet lifetimes of 0.3 μs while that of **14** has not been reported earlier.[23] As a result, the isoprene photodimerizations using dinaphthylmethanone sensitizers can be run with very low sensitizer loadings and as they absorb solar irradiation, it is apparent that particularly **12** is a suitable sensitizer.

The yields of isoprene dimers when xanthone **10** and thioxanthone **11** were used as photosensitizers were significantly lower as compared to when benzophenone was used, and we initially considered this to arise from their poor solubility in neat isoprene. To improve the solubility, we designed and synthesized 3,6-di(octyloxy)xanthenone (**15**) with solubilizing alkyl groups (for synthesis see ESI†). Yet, despite an improved solubility, the improvement in the isoprene-to-dimer conversion is minute (from 8 to 11%). Instead, the higher $E(T_1)$ of both **10** and **15** compared to **9** may cause less efficient triplet energy transfer and, consequently, a less efficient isoprene dimerization. Indeed, the calculated triplet energy of **15** is higher than that of **10** by nearly 3 kcal/mol, revealing that substitution allows for further tailoring of xanthone-type sensitizers, similarly as recently reported by Booker-Milburn and co-workers.[29]

Table 1 Photosensitizer screening for the isoprene photodimerization performed in quartz test tubes in a Rayonet photoreactor.

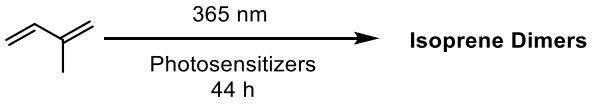

Photosensitizer	**Loading of photosensitizer (mol%)**	**Isolated yield (%)**
No photosensitizer	0	0.5
9	2	36

10	(0.4)[a]	8
11	(0.1)[a]	26
12	(0.5)[a]	41
13	(0.3)[a]	34
14	(0.3)[a]	21
15	2	11

[a] The actual loading was lower due to poor solubility of the sensitizer in isoprene.

Optimization of dinaphthylmethanone sensitized dimerization: Having identified the most suitable photosensitizers among those selected, we determined the loading of **12** required for the optimal conversion of isoprene to its dimers. The photosensitizer loadings were screened from 0.5 down to 0.01 mol% with a similar setup as used above (see Table S2, ESI†). We could observe 21% yield of isoprene dimers in 44 h with the loading of **12** as low as 0.01 mol%. It is worth noting that the yield of the isoprene dimers does not correlate linearly with the loading of **12** as the light transmission through the solution likely influences the yields. We found that a loading of **12** of 0.1 mol% was adequate to get an optimized yield of the isoprene dimers.

Further improvement of the photodimerization was carried out in modified reaction setups. We first used a Teflon™ tubing (outer diameter: 3.2 mm) coiled (~20 mL loop size) around a water-cooled condenser (Fig. S12, ESI†). The Teflon tubing setup extensively increased the surface area for the incident light, which in turn improved the light absorption. The water-cooled condenser also allows the reaction to run at ~10 ºC which prevents evaporation of the volatile isoprene. With this setup and with 0.1 mol% of loading of **12**, we observed 91% yield of isoprene dimers (20 mL scale) when photo-irradiated for 44 h. The isomer distribution between the isoprene dimers, as quantitatively determined through the ^{1}H

NMR spectrum, were found to be: **2** (16.1%), **3** (16.5%), **4** (10.7%), **5** (20.8%), **6** (21.8%), and **7** and **8** (14%) (Fig. S13, ESI†). Therefore, the major fraction of the dimers consists of [2+2] isoprene cycloadducts (43.3%), in accordance with the ratios observed by Liu et al.[18] The lower triplet energy of dinapthylmethanone **12** than of **9** leads to preferential activation of *s-cis* isoprene, resulting also in high amounts of [4+2] cycloadducts (42.6%). The isoprene dimers and photosensitizer **12** could easily be separated by passing through a short silica gel column by using pentane as eluent or by distillation under reduced pressure (65 ºC at ~0.1 mmHg).

The isoprene dimers could be stored at 4 °C for a few months without noticeable decomposition (Fig. S14, ESI†). However, the conversion of kinetically stable [2+2] photodimers to the other thermodynamically more stable dimers was observed after a few months in storage (Fig. S15, ESI†) or upon heating over 100 °C. Also noteworthy is that under ambient conditions the photodimers tend to convert slowly over time to the corresponding immiscible epoxides and alcohols (Fig. S16-17, ESI†).

Now, can the photochemical formation of isoprene dimers be run under ambient atmosphere? To explore this, we analysed the photodimerization with the aforementioned setup and photosensitizer content for 44h under ambient conditions and observed the same yield (92%) as before. The improved photosensitizing efficiency of **12** compared to benzophenone **9** is attributed to the higher absorption at 365 nm (Fig. S10, ESI†), lowest triplet energy difference as well as higher photodimerization quantum yield (ϕ = 0.91 for the dinaphthyl methanone **12** versus ϕ = 0.43 for benzophenone **9**, see ESI† for details). It is also noteworthy that **12** is straightforwardly synthesized in a one-pot reaction using cheap reagents, and after the photoirradiation it can easily be recovered, purified, and used for another cycle. Finally, very low amounts of **12** as photosensitizer (0.1 mol% loading) are needed, which together with its recyclability, should significantly reduce the cost for large-scale production of isoprene dimers.

Dimerization induced by (simulated) solar irradiation: Our ultimate goal is to carry out the photodimerization of isoprene with solar irradiation (Fig. S20, ESI†). Dinaphthylmethanone **12** might be an ideal photosensitizer as its absorption tail stretches until ~400 nm and the solar irradiation has significant light intensity at the surface of Earth at wavelengths longer than 350 nm (Fig. S21, ESI†). For this reason, we first performed the isoprene photodimerization in a solar simulator (AM 1.5G) using a newly designed flat spiral coil made of Teflon tubing for simulated solar irradiation of isoprene (Fig. 4). Now, we could see 61% yield of isoprene dimers (4 mL scale) when irradiated in the solar simulator for 44 h using 0.1 mol% of dinaphthylmethanone **12** as photosensitizer (Fig. S22, ESI†).

Using the flat spiral coil and 0.1 mol% of **12**, the isoprene dimerization was also tested outdoors in sunlight (Uppsala, Sweden 59°51'09.5"N 17°39'19.9"E, approximately 30 m above sea level on May 30 - 31, 2020). In this experiment we observed 17% yield after a total exposure time to the sun of 20 h (Fig. S23-24, ESI†). This result is qualitative since reduction in light intensity due to clouds was not considered and as the solar light intensity varies over the day. Thus, the experiment demonstrates that the formation of isoprene dimers under sunlight irradiation is achievable. Furthermore, the higher yield that can be estimated after 20 h in the solar simulator (28%) can be rationalized by the fact that the solar simulator in the 350 – 400 nm interval has an intensity which is approximately double that of incident solar light corresponding to one sun (see Fig. S21, ESI†).

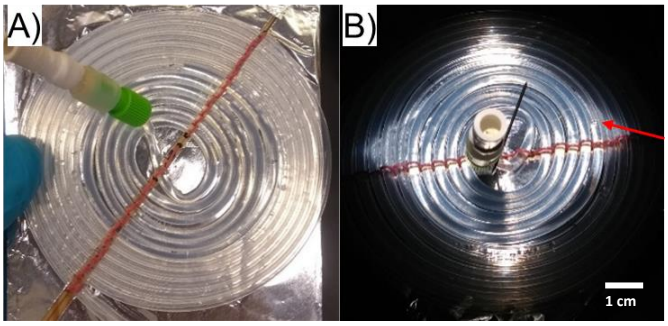

Fig. 4 A) The custom-made setup with a coiled Teflon tubing (O.D. × I.D. : 3.18 mm × 2.1 mm, 10 cm diameter) on a flat surface for solar simulator and solar irradiation of isoprene. B) The isoprene being photoirradiated by the solar simulator. The arrow indicates the filling level of isoprene.

Photodimerization of bio-isoprene: The bio-isoprene produced by the *Synechocystis* cells and captured in heptane was mixed with dinaphthylmethanone **12** (0.02 M), filled into the flat spiral coil and irradiated in the solar simulator (24 h, 1 sun, AM 1.5 G). Even though the concentration of bio-isoprene was low, the reaction produced bio-isoprene dimers as confirmed by GCMS (Fig. 5), and experiments with commercially available isoprene (0.05 M solution in heptane) gave a similar distribution pattern of dimers (Fig. S25-26, ESI†). This proof-of-principle experiment shows the possibility to turn CO_2 used as carbon source into C_{10} cycloalkanes with our combined photobiological-photochemical approach. Bio-isoprene dimerization was also attempted under natural sunlight, yet, no dimer formation was observed in this case. This contrasting result when compared to the solar simulator experiment is likely due to two factors; (*i*) the weaker intensity of the natural solar light compared to the simulated one in the 350-400 nm range (Fig. S21, ESI†) and (*ii*) the low concentration of the bio-isoprene in heptane. Thus, one next step is to increase the production of bio-isoprene so that a higher concentration can be achieved. This may be addressed via further metabolic engineering of the cyanobacterial strain to enhance flux of fixed carbon towards the isoprene product.

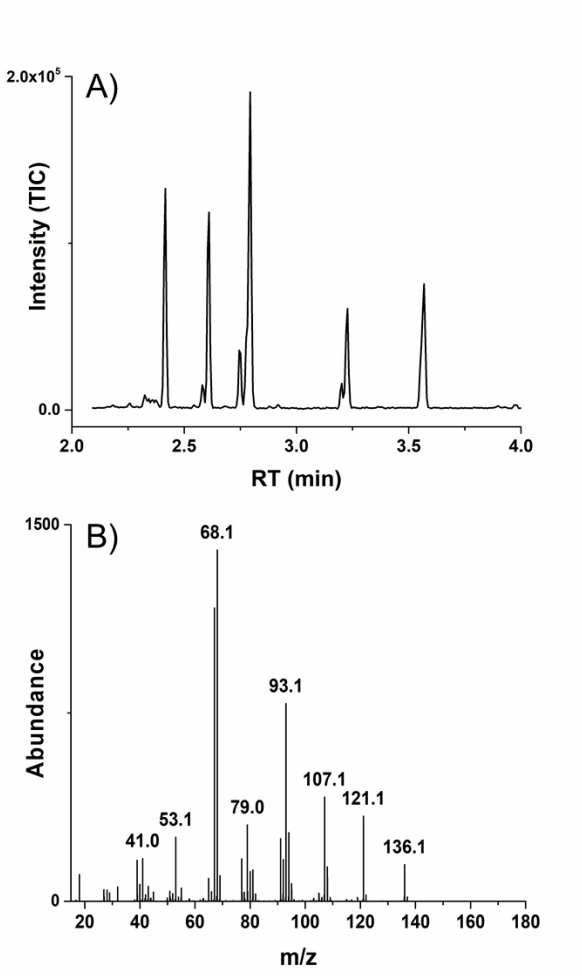

Fig. 5 A) Gas chromatogram showing peaks of bio-isoprene dimers (for the relationship between peaks and isomer types and full chromatograms, see Fig. S25, ESI†). B) The average mass spectrum for the region RT = 2.392 to 3.623 min, for bio-isoprene solution in heptane. The reaction was photosensitized by dinaphthylmethanone **12** (0.02 M, heptane). The sample was irradiated under simulated sunlight, Xenon lamp (1 sun, AM 1.5 G, 24 h, flat spiral coil).

Photodimerization mechanism: The reaction mechanism for light-induced formation of the isoprene dimers observed involves five steps (steps 1- 5, Fig. 6) as confirmed through computations (for details see the ESI†). The first step is the excitation and intersystem crossing (ISC) of the photosensitizer to its triplet state, followed by triplet energy transfer from the sensitizers to isoprene in the ground state yielding isoprene in its T_1 state. The T_1 state isoprene can be described as one allyl radical and one methyl radical, and the lowest activation

energies for the addition of the methyl radical site to an S_0 isoprene molecule are ~50 kJ/mol (step 3), while the addition of the allyl radical part to an S_0 state isoprene proceeds over a slightly higher barrier of ~63 kJ/mol. The triplet lifetime of isoprene has been determined to 5 μs,[18,30] sufficiently long to allow a substantial amount to overcome the activation barrier for dimerization. The addition leads to *bis*(allyl) radical pairs with overall triplet multiplicity and this dimerization step is markedly exergonic (-92 to -71 kJ/mol). As the two radical sites of the *bis*(allyl) radical pair are only weakly interacting, the singlet diradical is essentially isoenergetic with the triplet, and a rapid ISC occurs (step 4). Additionally, the *bis*(allyl) radical pair has a high conformational flexibility irrespective of which electronic state it is in as the conformer interconversion involves C-C single bond rotations (in the T_1 state the rotational barriers are ~13 kJ/mol). Thus, when oriented appropriately the two unpaired electrons of the singlet *bis*(allyl) radical pair will combine into a C-C single bond (step 5), leading to the observed isoprene dimers with cyclobutane, cyclohexene and cyclooctadiene rings (Fig. 1C).

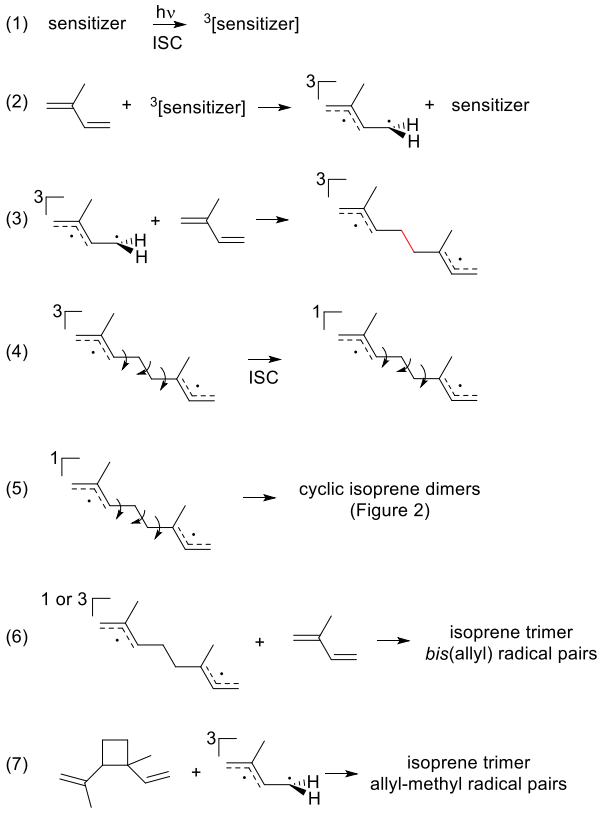

Fig. 6 The various steps in the reaction mechanism for the formation of the cyclic isoprene dimers (steps 1 to 5) and trimers (steps 6 and 7). ISC = intersystem crossing. For details see the Supporting Information.

So why is further oligomerization hampered? As the *bis*(allyl) radical pairs are composed of two allyl radicals which are internally stabilized through π-conjugation, they will be less reactive than triplet state isoprene which is composed of one allyl radical and one reactive methyl radical fragment orientated perpendicularly relative to each other. Thus, the rate for the addition of the *bis*(allyl) radical pair to an isoprene in its S_0 state, leading to a trimer *bis*(allyl) radical pair, should be slow (step 6). Indeed, the lowest activation barrier for the addition of the *bis*(allyl) radical pair to an S_0 state isoprene is 92 kJ/mol, significantly higher than the addition of a T_1 state isoprene to an S_0 state isoprene (50 kJ/mol as seen above). A second potential route to trimers goes via addition of an T_1 state isoprene to a C-C double bond of a cycloadduct, but this process should also be slow as it leads from a single carbon-centered radical to another (step 7). For this process we find a lowest calculated activation energy of 79 kJ/mol. Combined, this explains why the further oligomerization is not competitive with the closure of the *bis*(allyl) radical pair to the cyclic dimers observed.

Finally, since the combined portions of isoprene dimers that are either [2+2] and [4+4] cycloadducts make up more than half of the dimer mix, we also tested a T_1 state concerted mechanism that would involve a transition state with a cycle of 4*n* electrons stabilized by through-space Baird-aromaticity,[31–33] yet, we could not find such a pathway. For further discussions, see ESI†.

Hydrogenation and fuel performance: The isoprene dimers are unsaturated, which is not ideal if they should function as a jet fuel as soot would form due to incomplete combustion when ignited. The isoprene dimers (here labelled **ID-1**) were therefore

hydrogenated in a Parr hydrogenation apparatus in presence of Pd/C as a catalyst at 10 atm hydrogen pressure, providing hydrogenated isoprene dimers (**HID-1**) in near quantitative isolated yields (see ESI† for detail procedure). These hydrogenated isoprene dimers appeared as a colorless liquid (Fig. S27, ESI†), and they were further characterized by ^{1}H NMR spectroscopy and GCMS analysis (Fig. S28, ESI†). The disappearance of the alkene signals of the isoprene dimers in the ^{1}H NMR spectrum proves a complete reduction of the C-C double bonds, leading us to the cycloalkane-based jet fuel equivalent.

For this mixture of hydrogenated isoprene dimers, we determined the key fuel properties, *i.e.*, the net heat of combustion (NHOC), kinematic viscosity, density, and flash point (Table 2). The measured density of **HID-1** is 0.77 g/mL at 15 °C (Table S6 and Fig. S39, ESI†) which matches well with the lower required density of **Jet-A**. The density of the fuel is lower than that of dimethylcyclooctanes (**DMCO**) due to the presence of high amounts of isomers with cyclobutane rings. Moreover, the hydrogen content of the **HID-1** (14.37%) is significantly higher than that of **Jet-A** due to the absence of aromatic and unsaturated moieties, which eventually gives a higher gravimetric NHOC value and produce clean burn without soot formation. The gravimetric NHOC is an important parameter for a jet fuel, and it should be above 42.8 MJ/kg according to the standard specification for jet fuels.[15] Additionally, the volumetric NHOC value of **HID-1** is higher than that of conventional jet fuels (**Jet-A**). For the two C_{10} hydrocarbons (**18**, **19**, **25** and **26**) in Fig. 7 which have experimentally determined NHOC,[6,15] we find that the computed values are in good agreement. Thus, based on the computed NHOC of the $C_{10}H_{20}$ hydrocarbons contained in **HID-1** we can also conclude that their energy contents are in line with expected for an aviation fuel.

Table 2 Key ASTM (American Society for Testing and Materials) fuel properties of **HID-1**, **HID-2** and **HID-3** and of two existing aviation fuels.

Fuel Property	**HID-1**	**HID-2**	**HID-3**	**DMCO**[a]	**Jet-A**[a]
Gravimetric Net Heat of Combustion (NHOC), MJ/kg	44.23	43.57	43.59	43.82	>42.8
Density (15 ºC), g/mL	0.770	0.809	0.808	0.827	>0.775
Volumetric NHOC, MJ/L	34.05	35.25	35.22	36.22	>33.17
Kinematic viscosity (-20 °C), mm^2/s	1.71	3.16	2.92	4.17	<8.00
Freezing point, °C	<-78	<-78	<-78	<-78	<-40
Flash point, °C	33.5	38.5	38.5	50	>38
Hydrogen content, % mass	14.37	14.37	14.37	---	>13.4

[a] ASTM specification for Jet-A. Data taken from Ref. No. 15.

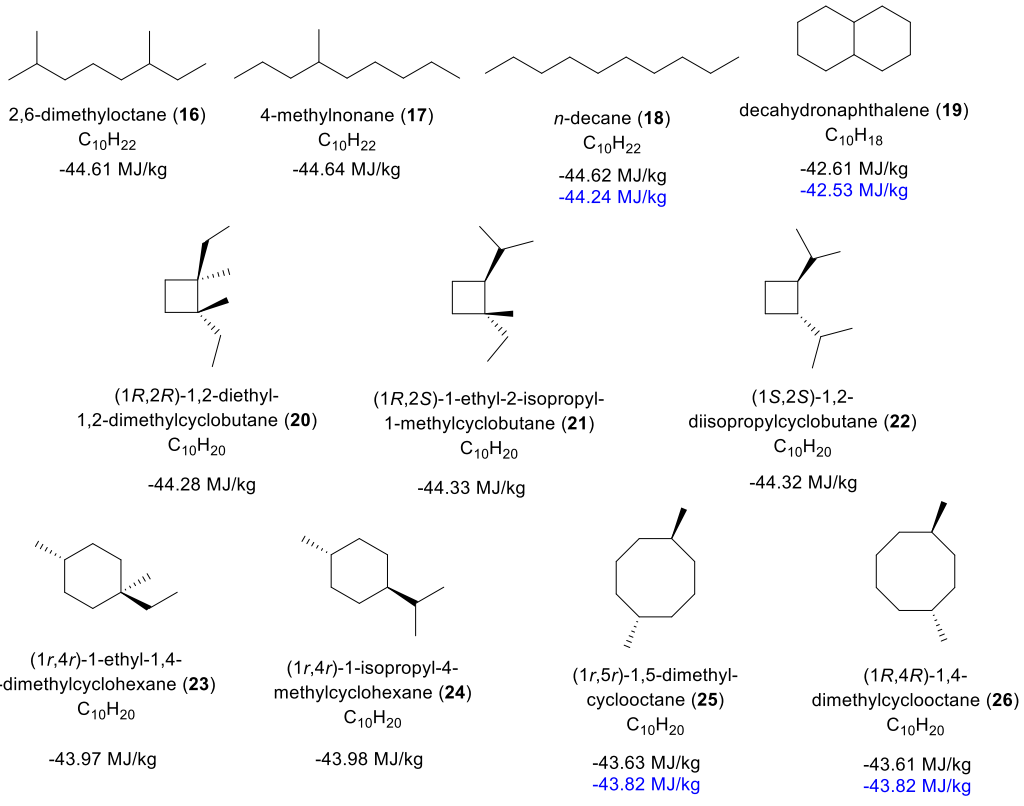

Fig. 7 Computed and experimentally determined net heat of combustion (NHOC) values for a few C_{10} hydrocarbons that exist in **HID-1** and in the **Jet-A** fuel. Experimental values from ref. 6 (compounds **18** and **19**) and ref.15 (compounds **25** and **26**, determined as a 1:10 mixture) The NHOC values were computed following the procedure described by Major and co-workers.[34]

Additionally, we have measured the kinematic viscosity of **HID-1** from -40 °C to 20 °C as it is an important parameter in terms of safety and combustion of the fuel.[35] A higher viscosity leads to a poorer atomization of the fuel which leads to incomplete combustion and formation of soot, eventually reducing fuel efficiency. To achieve proper atomization and combustion of a jet fuel it is strongly recommended to have a kinematic viscosity value below 12.00 mm^2/s at -40 °C. Rewardingly, the kinematic viscosity of **HID-1** (1.71 mm^2/s at -20 °C) is more than 4.5 times lower than the recommended value for conventional fuel (8.00 mm^2/s), and it is even 2.4 times lower than that recently reported for **DMCO** (4.17 mm^2/s at -20 °C) which is closely related to the structure of the molecule (C_{10}). The kinematic viscosity at -40 °C is 2.60 mm^2/s (Table S4 and Fig. S38, ESI†), which is 4.6 and 3.1 times lower compared to **Jet-A** and **DMCO** (7.95 mm^2/s), respectively. The lower kinematic viscosity might result from the higher portion of alkylated cyclobutane isomers over cyclooctane isomers, and it will allow the drop-in to be blended with other conventional jet fuels at any ratio.

The freezing point of the jet fuel is also crucial for the safety and the flow of the fuel at high altitudes. We assessed the freezing properties of **HID-1** by placing it in a dry ice/acetone bath (-78 °C) for 1.5 h and did not observe any cloudiness or crystallization, indicating that the freezing point of **HID-1** is lower than -78 °C, *i.e.*, it is much lower than the recommended value for conventional jet fuel (-40 °C). The low freezing point of **HID-1** suggests that it is possible to use as a fuel in high altitude flight. Yet, a drawback of **HID-1** is the flashpoint which was found to be 33.5 °C, lower than the specified value for conventional

jet fuel (38 °C). The lower flash point may limit the use of **HID-1** as jet fuel surrogate due to safety issues, although the commercially available **Jet-B** and **TS-1** have much lower flash points (-18 and 28 °C, respectively) compared to the recommended value.[36] Yet, these fuels have very low freezing points allowing them to be used in extremely cold environments. The low flash point of **HID-1** can be attributed to the isomers with cyclobutane rings as these are more volatile.

Further modification of the C_{10} fuel: The fact that the flash point is slightly below the recommended value prompted us to consider modifications of the isoprene dimer mix **ID-1** before the hydrogenation step. The boiling points of the various isomeric isoprene dimers (**2** - **8**, Fig. 1C) were earlier reported by Hammond, Turro and Liu and it was revealed that the [2+2] isomers have lower boiling points than the others (Fig. S13, ESI†),[17] with **2** having the lowest. This should also contribute to the low flash point of **HID-1** as the flash point of a hydrocarbon correlates with its vapor pressure. A further modification of **ID-1** could be performed through moderate heating which led to the conversion of cyclobutane-containing isomers to cyclooctadiene- and cyclohexene-containing ones through Cope and other thermal rearrangements.[17] Here we probed two different temperatures, 135 and 160 °C, and subsequent hydrogenation gave the modified hydrogenated isoprene dimers **HID-2** and **HID-3** (Fig. 8). The reaction mixtures were analyzed by ^{1}H NMR and GCMS measurements (Fig. S29-32, ESI†).

When **ID-1** is heated at 135 °C for 1.5 h, leading to **ID-2**, the isomer **2** rearranges to isomers **5** and **8**, although a drawback is the re-formation of isoprene as a byproduct to ~5 % (Fig. S33, ESI†). In order to transform all [2+2] isoprene dimers into [4+2] and [4+4] isomers the temperature had to be elevated to 160 °C for 4 h, giving **ID-3**. Yet, in this case the amount of isoprene formed through a back-reaction increased to ~11 %, even though **3** and **4** after prolonged heating remained in the post-modified **ID-3** in trace amounts of ~1 and ~2 %,

respectively (Fig. S34, ESI†). After removal of isoprene from **ID-2** and **ID-3**, these dimer mixtures were hydrogenated using the conditions described above leading to quantitative formation of **HID-2** and **HID-3** (Fig. S35-37, ESI†). It is worth noting that the post-modification of **ID-1** can be justified, as the isoprene formed as a byproduct can be recycled.

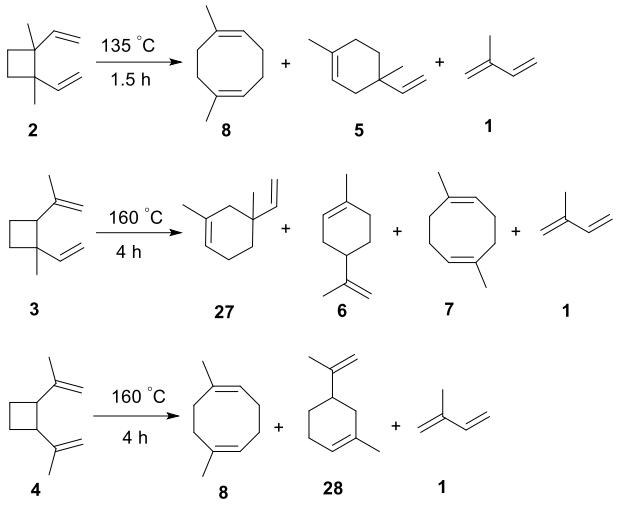

Fig. 8 Isomerization of the cyclic [2+2] isoprene dimers to plausible cyclic [4+4] and [4+2] isomers through thermal Cope and other rearrangements.

After the heat treatments, the flash points of **HID-2** and **HID-3** increased to 38.5 °C (Table 2), *i.e.*, above the recommended value. The identical flash point of **HID-2** and **HID-3** can be rationalized as they are mixtures of hydrogenated cycloalkanes with very similar boiling points. The gravimetric NHOC values of **HID-2** and **HID-3** decreased to 43.57 and 43.59 MJ/kg, respectively, lower than that of **HID-1** which is explained by the reduced amounts of cyclobutane isomers in the modified **HID** blends. Yet, the modified **HID**'s have higher densities (both 0.809 g/mL at 15 °C) (Table 1, S6 and Fig. S39, ESI†) which leads to higher volumetric NHOC values (35.25 and 35.22 MJ/L, respectively). The volumetric NHOC values for modified fuels are 6.3% greater compared to conventional **Jet-A** (> 33.17 MJ/L), which should be an added advantage. With regard to the kinematic viscosities (3.16 and 2.92 mm^2/s

at -20 °C for **HID-2** and **HID-3**, respectively) these are higher than that of **HID-1** due to their lower contents of cyclobutanes (Table 1, S4 and Fig. S38, ESI†). Still, the values are more than 2.5 times lower than the largest recommended values, facilitating a good atomization of the **HID**'s when used as fuels. Finally, both modified fuels have very low freezing points (<-78 °C), enabling high altitude flight (Table 1). The easy modulation of the **ID-1** to **ID-2** and **ID-3** should be an advantage as they after hydrogenation should be ideal as drop-ins for conventional fuels for high-altitude jet engines.

There are also further favourable features of **HID-1** – **HID-3**. Conventional jet fuels contain mixtures of aromatic compounds which have added benefits as they swell the nitrile rubber elastomer valves which helps to protect the integrity of the jet engine. However, modern elastic materials do not require the aromatic fuel content to swell the elastomers, and recent studies have shown that cycloalkane blends have similar properties as aromatics and are able to swell nitrile rubber elastomer valves.[37,38] Additionally, the content of aromatic compounds in jet fuels leads to lower NHOC values as well as formation of carbon soot during the combustion which adversely affects the lifetime of the engine. Finally, aromatic compounds in jet-fuels are major health and environmental hazards. Thus, avoidance of such compounds is favorable for these reasons, and substantial interests have been focused towards development of bio-cycloalkane based fuels that mitigate the abovementioned problems.[39] The very recent review by Muldoon and Harvey further highlights the potential of bio-cycloalkane based hybrid fuels for future use in military and civilian aviation fuel industries.[39] In this context it can be noted that JP-10 (exo-tetrahydrodicyclopentadiene) is a synthetic C_{10} cycloalkane-based missile fuel.[40,41] Taken together, our jet fuel mixtures (**HID-1** to **HID-3**), which are C_{10} cycloalkanes, fulfil all requirements for future, less environmentally hazardous jet fuels, they are devoid of aromatic content and have high NHOC values.

Conclusions and Outlook

In this study, we demonstrated that it is possible to generate photosynthetically derived isoprene from engineered cyanobacteria, capture the isoprene, and use it for subsequent biofuel generation via photochemical processes. While further optimization of the engineered microorganisms is required for industrial applications, we were able to trap isoprene with high efficiencies relying on a simple capturing method (that can be easily scaled up). Since the capture can be performed without compromising the sterility of the culture, one can perform several cycles of isoprene production and trapping on the same culture.

In a subsequent photochemical step, the isoprene was dimerized into cyclic $C_{10}H_{20}$ isomers in nearly quantitative yields by usage of dinapthylmethanones as photosensitizers. The photoreaction could be run under ambient conditions, facilitating a fully renewable fuel production. Our current studies reveal that rather simple modifications of the reaction setup can greatly improve the yield of the photoreaction. Combined with a careful choice of photosensitizer this enables photodimerization of isoprene by use of solar light. The isoprene dimer mixture can be further modified by heating at moderately elevated temperatures (130 – 160 °C), resulting in C_{10} hydrocarbon mixtures which after hydrogenation fulfil all criteria to function as drop-ins for conventional jet fuels. Indeed, the modified and hydrogenated isoprene dimers have better fuel properties than the commercially available Jet-A. The very low freezing points and low viscosity should make these fuels ideal for high-altitude flights.

The results described are the very first steps toward a completely renewable jet fuel generated from CO_2, water and solar light, provided that cultivation is carried out outdoors and that the hydrogenation and thermal rearrangement steps also utilize renewable energy. We report on the first proof-of-principle study of a combined photobiological-photochemical approach for jet fuel production. Extensive future research and development along various lines are needed, and several different short alkenes and dienes could be useful for similar processes.

In the photochemical dimerization of isoprene presented in this study, we have produced in total ~400 ml of hydrogenated monoterpenes. In an estimation, this amount would allow an Airbus A380 to fly (at least) ~22 m based on the fact that it is estimated to burn 13.78 kg/km and that the densities of our fuels are ~0.8 g/mL.[42] Considering this, there is a very long way to go before we have reached fully sustainable jet fuels produced by a combined photobiological-photochemical approach. Yet, every journey begins with a single step.

Conflicts of interest

There are no conflicts of interests.

Acknowledgements

First, we are grateful to Dr. Per Wiklund for helping out in establishing the contact between HO and MB, which enabled us to determine the fuel characteristics, Dr. Wangchuk Rabten for design and construction of the flat tubing reactor, Dr. Luke Odell for proving access to GC-MS, Prof. Johannes Messinger for access to the solar simulator, and Prof. Máté Erdélyi and Dr. Ruisheng Xiong for access to their Parr hydrogenation apparatus. Financial support from The Swedish Energy Agency (grants 44728-1 (HO) and 38334-3 (PiL)) and Formas (grant 2017-00862) are greatly acknowledged. The computations were enabled by resources provided by the Swedish National Infrastructure for Computing (SNIC) at the National Supercomputer Center (NSC), Linköping, partially funded by the Swedish Research Council through grant agreement number 2016-07213.

Author contributions: The photobiological production of isoprene has been carried out by JR, the trapping by JR and JS, the photochemical dimerization, optimization of reaction conditions, spectroscopic and chemical analysis, and hydrogenation by AR, LCG and HAV, quantum

chemical calculations by NPV, OEB and AR, and determination of fuel properties by LA and MB. The two-step combined photobiological-photochemical approach was conceived by HO, KS, PiL and PeL, and the application to isoprene dimerization by PiL and HO. All authors have contributed to the writing of the manuscript.

References

1 International Air Transport Association (IATA), *Aircraft Technology Roadmap to 2050*, 2019.

2 A. de Juniac, *International Air Transport Asscіation Annual Review 2019*, 2019.

3 J. Zhou, T. Zhu, Z. Cai and Y. Li, *Microb. Cell Fact.*, 2016, **15**, 1–9.

4 Air BP, *Handbook of Products*, 2011.

5 G. Coordinating Research Council (CRC): Alpharetta, *Handbook of Aviation Fuel Properties CRC Report No. 635*, 2004.

6 B. L. Smith and T. J. Bruno, *Energy and Fuels*, 2007, **21**, 2853–2862.

7 N. R. Baral, O. Kavvada, D. Mendez-Perez, A. Mukhopadhyay, T. S. Lee, B. A. Simmons and C. D. Scown, *Energy Environ. Sci.*, 2019, **12**, 807–824.

8 P. P. Peralta-Yahya, M. Ouellet, R. Chan, A. Mukhopadhyay, J. D. Keasling and T. S. Lee, *Nat. Commun.*, 2011, **2**, 483.

9 C. L. Liu, T. Tian, J. Alonso-Gutierrez, B. Garabedian, S. Wang, E. E. K. Baidoo, V. Benites, Y. Chen, C. J. Petzold, P. D. Adams, J. D. Keasling, T. Tan and T. S. Lee, *Biotechnol. Biofuels*, 2018, **11**, 1–15.

10 P. Lindberg, S. Park and A. Melis, *Metab. Eng.*, 2010, **12**, 70–79.

11 H. Mustila, A. Kugler and K. Stensjö, *Metab. Eng. Commun.*, 2021, **12**, e00163.

12 X. Gao, F. Gao, D. Liu, H. Zhang, X. Nie and C. Yang, *Energy Environ. Sci.*, 2016, **9**, 1400–1411.

13 E. Englund, K. Shabestary, E. P. Hudson and P. Lindberg, *Metab. Eng.*, 2018, **49**, 164–177.

14 C. P. Nicholas, *Appl. Catal. A Gen.*, 2017, **543**, 82–97.

15 K. E. Rosenkoetter, C. R. Kennedy, P. J. Chirik and B. G. Harvey, *Green Chem.*, 2019, **21**, 5616–5623.

16 D. M. Morris, R. L. Quintana and B. G. Harvey, *ChemSusChem*, 2019, **12**, 1646–1652.

17 G. S. Hammond, N. J. Turro and R. S. H. Liu, *J. Org. Chem.*, 1963, **28**, 3297–3303.

18 R. S. H. Liu, N. J. Turro and G. S. Hammond, *J. Am. Chem. Soc.*, 1965, **87**, 3406–3412.

19 R. Satthawong, N. Koizumi, C. Song and P. Prasassarakich, *J. CO2 Util.*, 2013, **3**–**4**, 102–106.

20 C. Vogt, M. Monai, G. J. Kramer and B. M. Weckhuysen, *Nat. Catal.*, 2019, **2**, 188–197.

21 B. Yao, T. Xiao, O. A. Makgae, X. Jie, S. Gonzalez-Cortes, S. Guan, A. I. Kirkland, J. R. Dilworth, H. A. Al-Megren and S. M. Alshihri, *Nat. Commun.*, 2020, **11**, 6395.

22 J. S. Rodrigues and P. Lindberg, in *Cyanobacteria Biotechnology*, ed. E. P. Hudson, Wiley, 2021.

23 S. K. Rajagopal, K. Nagaraj, S. Deb, V. Bhat, D. Sasikumar, E. Sebastian and M. Hariharan, *Phys. Chem. Chem. Phys.*, 2018, **20**, 19120–19128.

24 S. V. Jovanovic, D. G. Morris, C. N. Pliva and J. C. Scaiano, *J. Photochem. Photobiol. A Chem.*, 1997, **107**, 153–158.

25 S. L. Murov, Ph.D. Thesis, Univ. Chicago, Chicago, IL, 1967.

26 J. P. Fouassier, D. J. Lougnot, F. Wieder and J. Faure, *J. Photochem.*, 1977, **7**, 17–28.

27 K. Meier and H. Zweifel, *J. Photochem.*, 1986, **35**, 353–366.

28 G. S. Hammond and R. S. H. Liu, *J. Am. Chem. Soc.*, 1963, **85**, 477–478.

29 L. D. Elliott, S. Kayal, M. W. George and K. Booker-Milburn, *J. Am. Chem. Soc.*, 2020, **142**, 14947–14956.

30 P. A. Leermakers, J.-P. Rauh and R. D. Montillier, *Mol. Photochem.*, 1969, **1**, 57.

31 N. C. Baird, *J. Am. Chem. Soc.*, 1972, **94**, 4941–4948.

32 K. Jorner, B. O. Jahn, P. Bultinck and H. Ottosson, *Chem. Sci.*, 2018, **9**, 3165–3176.

33 V. Vijay, M. Madhu, R. Ramakrishnan, A. Benny and M. Hariharan, *Chem. Commun.*, 2019, **56**, 225–228.

34 E. Pahima, S. Hoz, M. Ben-Tzion and D. T. Major, *Sustain. Energy Fuels*, 2019, **3**, 457–466.

35 G. R. Wilson, T. Edwards, E. Corporan and R. L. Freerks, *Energy and Fuels*, 2013, **27**, 962–966.

36 D. J. L. Prak, G. R. Simms, M. Hamilton and J. S. Cowart, *Fuel*, 2021, **286**, 119389.

37 J. L. Graham, T. F. Rahmes, M. C. Kay, J. P. Belières, J. D. Kinder, S. A. Millett, J. Ray, W. L. Vannice and J. A. Trela, *Impact of alternative jet fuel and fuel blends on non-metallic materials used in commercial aircraft fuel systems. Federal Aviation Administration Report DOT*, FAA/AEE/2014–10, 2014.

38 Y. Liu and C. W. Wilson, *Adv. Mech. Eng.*, , DOI:10.1155/2012/127430.

39 J. A. Muldoon and B. G. Harvey, *ChemSusChem*, 2020, **13**, 5777–5807.

40 T. Bruno, M. Huber, a Laesecke, E. Lemmon and R. Perkins, *Adv. Sci. Tech.*, 2006, **45**, 1–67.

41 H. S. Chung, G. S. H. Chen, R. A. Kremer, J. R. Boulton and G. W. Burdette, *Energy and Fuels*, 1999, **13**, 641–649.

42 E. Samunderu, in *Air Transport Management: Strategic Management in the Airline Industry*, Kogan Page, London, 2020, p. 352.